

## Article

# Framework for Holistic Online Optimization of Milling Machine Conditions to Enhance Machine Efficiency and Sustainability

Alexander Bott <sup>1,\*</sup>, Simon Anderlik <sup>1,†</sup>, Robin Ströbel <sup>1</sup>, Jürgen Fleischer <sup>1</sup> and Andreas Wortmann <sup>2</sup>

<sup>1</sup> wbk Institute of Production Science, Karlsruhe Institute of Technology (KIT), Kaiserstraße 12, 76131 Karlsruhe, Germany; simon.anderlik@kit.edu (S.A.); robin.stroebl@kit.edu (R.S.); juergen.fleischer@kit.edu (J.F.)

<sup>2</sup> Institute for Control Engineering of Machine Tools and Manufacturing Units (ISW), University of Stuttgart, Seidenstrasse 36, 70174 Stuttgart, Germany; andreas.wortmann@isw.uni-stuttgart.de

\* Correspondence: alexander.bott@kit.edu; Tel.: +49-1523-950-2643

† These authors contributed equally to this work.

**Abstract:** This study addresses the challenge of the optimization of milling in industrial production, focusing on developing and applying a novel framework for optimising manufacturing processes. Recognising a gap in current methods, the research primarily targets the underutilisation of advanced data analysis and machine learning techniques in industrial settings. The proposed framework integrates these technologies to refine machining parameters more effectively than conventional approaches. The research method involved the development of the framework for the realisation and analysis of measurement data from milling machines, focusing on six machine parts and employing a machine learning system for optimization and evaluation. The developed and realised framework in the form of a software demonstrator showed its applicability in different experiments. This research enables easy deployment of data-driven techniques for sustainable industrial practices, highlighting the potential of this framework for transforming manufacturing processes.

**Keywords:** machine tools; online optimization; energy efficiency; tool wear; surface quality; asset administration shell; cloud manufacturing; sustainable machining



**Citation:** Bott, A.; Anderlik, S.; Ströbel, R.; Fleischer, J.; Wortmann, A. Framework for Holistic Online Optimization of Milling Machine Conditions to Enhance Machine Efficiency and Sustainability. *Machines* **2024**, *12*, 153. <https://doi.org/10.3390/machines12030153>

Academic Editor: Angelos P. Markopoulos

Received: 17 January 2024

Revised: 15 February 2024

Accepted: 20 February 2024

Published: 23 February 2024



**Copyright:** © 2024 by the authors. Licensee MDPI, Basel, Switzerland. This article is an open access article distributed under the terms and conditions of the Creative Commons Attribution (CC BY) license (<https://creativecommons.org/licenses/by/4.0/>).

## 1. Introduction

The escalating consequences of climate change, underscored by the relentless rise in greenhouse gas emissions, have thrust the manufacturing sector into the spotlight for its significant energy consumption and environmental footprint. The pressing need to curtail these emissions and enhance energy efficiency presents a critical challenge and opportunity for industrial operations. It is, therefore, imperative to decrease the presence of harmful greenhouse gases to address climate change and alleviate its repercussions. The manufacturing sector, driven by a heightened energy demand, must conscientiously and responsibly manage its available resources, including energy. This leads to implementing more stringent guidelines, such as the greenhouse gas protocol [1]. Moreover, the continual rise in industrial electricity prices [2] progressively compels companies to curtail their energy usage. Consequently, companies need to be more vigilant in overseeing and enhancing their energy consumption, which is continually rising. These challenges necessitate innovative approaches to reduce energy consumption in milling operations, moving beyond traditional methods that focus on general milling parameters applicable across various machining operations [3]. Recent research in this area has demonstrated significant advancements. For example, a method for the online optimization of cutting parameters by creating component models, which incorporate total energy consumption by accounting for machine configuration, tool, material, and machining instructions, was developed [4]. These models are adjusted individually and optimized using a divide-and-conquer strategy, aiming for minimal energy usage. Similarly, other approaches focused on

optimizing milling parameters through an intelligent CNC controller that adjusts cutting parameters in real time based on sensor data, thereby reducing energy consumption and tool wear [5]. Additional extensions also address a cloud environment to monitor production and optimally distribute jobs, intending to enhance the determination of milling parameters for energy efficiency [6]. The positioning of the workpiece regarding energy consumption has also become a focus of current research with the target to develop an optimization model for workpiece positioning to minimize axis-specific energy consumption [7]. However, these approaches often lack a holistic perspective, failing to consider the inter-dependencies between various machining parameters and their cumulative impact on energy consumption and environmental sustainability. Determining the optimal milling parameters for each part could enable further savings. Poor milling conditions could be detected immediately by optimizing the machine during machining, for example, due to unfavourably selected NC parameters.

The aim of this paper is, therefore, to present a holistic framework for the optimization of machining parameters during milling. This framework involves an automatic online analysis of recorded measurement data during the machining of parts. Based on these analyses, key indicators are defined and calculated automatically to characterize energy consumption and machining conditions. These indicators then inform recommendations to reduce energy consumption or optimize other variables using a fuzzy control system. This approach allows for the easy optimization of the machining process under various aspects, leveraging machine learning and advanced data analysis to significantly enhance energy efficiency and sustainability in industrial manufacturing. This framework addresses the critical need for sustainable and optimized production processes in an era of increasing environmental and economic challenges, contributing to reducing the manufacturing sector's environmental footprint through improved energy management and efficiency.

## 2. State of the Art

### 2.1. Prediction of Surface Roughness during Milling

Surface roughness is a central parameter for evaluating the quality of the manufactured part. The correlations between machining parameters and surface quality are the subject of numerous papers. In the following, previous approaches to predicting surface quality will be described. A distinction is made between steel and aluminium as a material.

It is known from numerous studies that in milling, the most relevant factors are the cutting depth  $a_p$ , the feed  $f_z$ , and the spindle speed  $n$  (or the cutting speed  $v_c$  calculated from  $n$ ) [8]. Colak et al. [9] used an evolutionary algorithm to predict the surface quality during milling. A novel approach called “gene expression programming” was used. Hayajneh et al. [10] experimentally investigated the effect of different machining parameters on surface roughness in milling. The individual factors of the regression model were then determined based on the experimental results. Simunovic et al. [11] investigated the effect of different cutting parameters on surface roughness during the milling of aluminium alloys using experiments. A regression model was determined to predict the surface quality. It was found that the surface quality mainly depends on the feed rate and the cutting speed. Yeganefar et al. [12] used different methods to predict and optimize the cutting forces as well as the surface quality in milling: regression analysis, support vector regressions (SVR), artificial neural networks (KNN), and genetic algorithms. KNN and SVR were found to have better prediction accuracy than the regression model. Nguyen and Hsu [13] analysed the effect of different process parameters on surface roughness in machining SKD61 steel. The feed has the greatest effect on surface roughness, followed by the depth of cut and cutting speed. Alauddin et al. [14] developed a model to predict the surface roughness when milling 190BHN steel. It was investigated using the response surface method. It was found that feed rate has the greatest influence on surface roughness. S.D. Philip et al. [15] investigated the effects of various milling parameters on surface quality using the response surface method. Feed rate was identified as the parameter with the greatest influence on surface roughness. Zhang et al. [16] used the Taguchi method to investigate the effect

of various influencing factors on surface roughness during milling. A cubic regression model was developed based on the experimentally obtained data. Good model quality was achieved in the subsequent model validation with test data.

Table 1 shows an overview of the regression models presented in this chapter. The ranges of values investigated for the various cutting parameters and the material used are listed below.

**Table 1.** Averaged range of values of the cut parameters in the different publications.

| Paper | Cutting Speed $v_c$ | Tooth Feed $f_z$ | Cutting Depth $a_p$ | Material  |
|-------|---------------------|------------------|---------------------|-----------|
| [11]  | 41.5–150 m/min      | 0.01–0.02 mm/rev | 0.13–0.97 mm        | aluminium |
| [10]  | 45–90 m/min         | 0.025–0.2 mm/rev | 0.25–1.25 mm        | aluminium |
| [9]   | 23.5–47 m/min       | 0.025–0.2 mm/rev | 0.25–1.26 mm        | aluminium |
| [12]  | 30–120 m/min        | 0.01–0.1 mm/rev  | 1.0–2.0 mm          | aluminium |
| [16]  | 90–150 m/min        | 0.04–0.16 mm/rev | 1–2.5 mm            | steel     |
| [13]  | 25–75 m/min         | 0.1–0.3 mm/rev   | 0.2–0.6 mm          | steel     |
| [15]  | 31.41–62.83 m/min   | 0.04–0.2 mm/rev  | 0.4–1.2 mm          | steel     |
| [14]  | 22–40 m/min         | 0.1–0.52 mm/rev  | 0.6–1.4 mm          | steel     |

## 2.2. Prediction of Tool Wear during Milling

Analogous to the prediction of surface roughness in Section 2.1, tool wear will also be predicted by a regression model from the literature.

Palanisamy et al. [17] developed a regression model and an artificial neural network to predict tool wear in milling. The tool wear is determined based on the flank wear. The input parameters for the two models are cutting speed, feed rate, and cutting depth. The parameter space spans a cutting speed of 10 to 100 m/min, a tooth feed of 0.05 to 0.25 mm/tooth, and a depth of cut of 0.5 to 2.5 mm. Due to this large parameter space, a combination of several models, as in Section 2.1, is unnecessary.

## 2.3. Prediction of Energy Consumption

Ströbel et al. [7] developed a model to predict the energy consumption during milling for the individual axes. The machine behaviour is first predicted based on the NC code. The corresponding machining steps are then extracted from the NC code, and time series are calculated. In the next step, the process forces are simulated by a voxel simulation. This model is used to determine the entry  $\varphi_1$  and exit angle  $\varphi_2$  of the tool, as well as the cutting depth  $a_p$ , the contact width  $a_e$  of the tool, and the material removed in the time step. Based on these quantities, the cutting forces are calculated using Kienzle's model. Finally, the energy consumption is predicted as current values for the individual axes based on the determined variables. The input variables of the network are the acceleration  $a_i$  and velocity  $v_i$  for all four axes, the calculated forces in all three spatial directions, and the spindle force. Furthermore, the material removal rate is relevant [7].

## 2.4. Use of Fuzzy Logic for Optimization Problems

Fuzzy logic for optimizing milling conditions is the subject of numerous scientific publications. Due to the description of the quantities by fuzzy membership functions, these systems apply to many problems. The following shows selected research results on this topic.

Xu et al. [18] used a so-called “novel adaptive neuro-fuzzy interference system” (NAN-FIS) to reduce energy consumption and optimize surface quality in a high-speed milling process. In this approach, a neural network is combined with a fuzzy system. First, the fuzzy system converts the input variables into linguistic variables before being processed by the neural network. The input variables of this model are the cutting parameters, and the output variables describe the machine's performance. It was found that cutting speed has one of the most significant influences on energy consumption. Gupta et al. [19] optimized turning operations at high speeds using a Taguchi fuzzy model. The optimization variables

are surface quality, tool wear, cutting forces, and energy consumption. A fuzzy system is used to combine various evaluation characteristics. Fuzzy membership functions describe the loss function. A rule base links the four input variables to the output variable. This output variable is called the “Comprehensive Output Measure” (COM). Yang et al. [20] used fuzzy particle swarm optimization to determine the optimal milling parameters in a multilayer milling operation. The parameters to be optimized are the number of paths, depth of cut, cutting speed, and feed rate. For this purpose, optimization is performed using a fuzzy particle swarm. The fuzzy system determines the speed for each individual. This procedure was validated through case studies, and it was shown that the optimal milling parameters can be determined efficiently with this procedure.

### 2.5. Milling Machine Used

The measurement data used in this thesis were recorded in [7]. For this purpose, milling tests were carried out on a CMX 600 V milling machine from the manufacturer DMG Mori. The machine is controlled utilizing a SIEMENS 840d control system. Via a SINUMERIK Edge Device, data from the control of the machine are tapped and stored in JSON files. The measured value records of four different parts are available. The training and validation parts were each made of steel and aluminium as materials, shown in Figure 1. The materials used are aluminium of type AL2007 and mild steel of type S235JR. The milling tools used have diameters of 5 mm, 10 mm, and 20 mm. A solid carbide milling cutter was used for the steel parts. An HSS milling cutter was used for the aluminium parts [7].

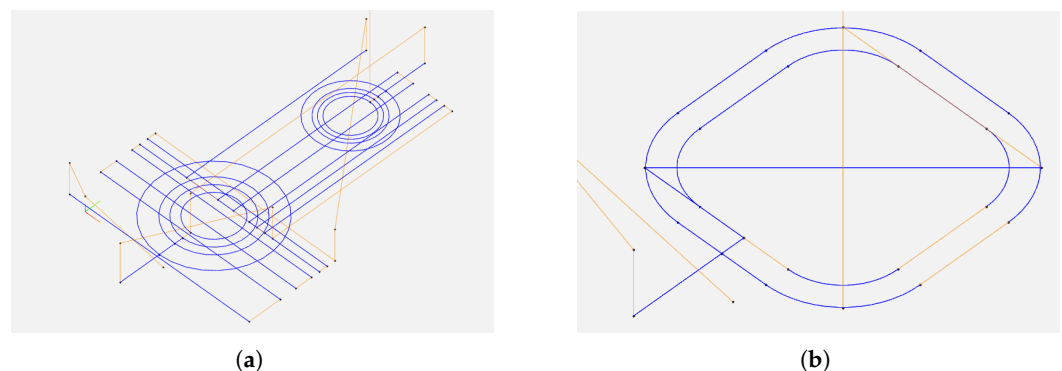


**Figure 1.** Simulation of the NC code for the different test parts. (a) Training part [21]. (b) Validation part [22].

### 3. Framework for Holistic Online Optimization

A framework for the machine data was developed for this purpose. The schematic structure of the framework is shown in Figure 2. At the beginning are the milling machine’s real-time machine data. SIEMENS Industrial Edge provides these. All measured variables available from the machine control system are recorded. The position data of all four axes and their variables, such as speed and acceleration, are particularly relevant for further analyses. In addition, the current values of the individual axes are required for comparability between the predicted and actual values. The received measurement data are time-stamped and transferred to the server via a network socket. This can be outsourced to a cloud environment. The individual components of the framework run in their own Docker containers, which achieves a modular structure, and the individual applications are independent of the host system.

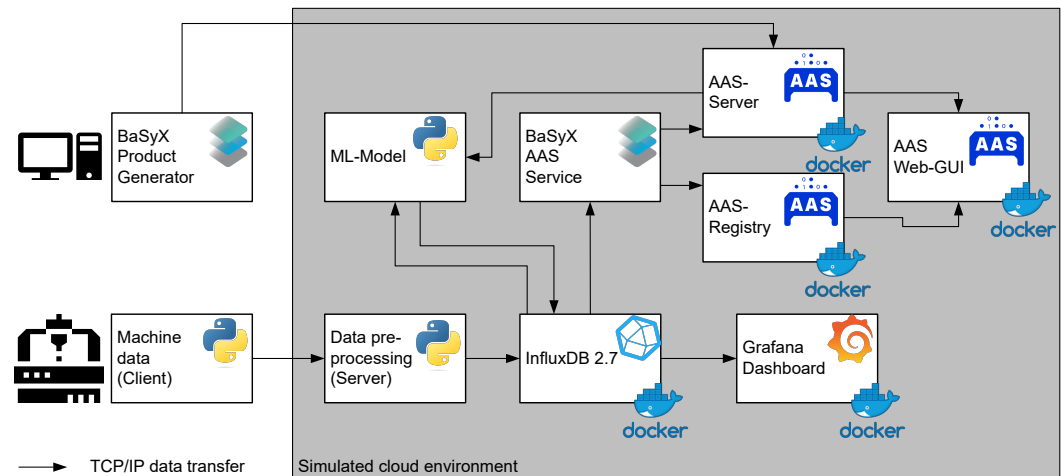


**Figure 2.** Schematic structure of the framework.

The server processes the received data. These are temporarily cached and stored in an Influx database in the next step. The sampling rate is reduced from 500 Hz to 50 Hz to minimize the amount of data. The maximum spindle speed within the test data is 7600 rpm. At a sampling rate of 50 Hz, the time interval between two data points corresponds to a maximum of approx. 2.5 spindle revolutions. As only the individual machining steps of the NC code are considered in this work, this sampling rate is sufficient, as a machining step is longer than 2.5 spindle revolutions. Subsequently, the measurement data are divided into segments corresponding to the individual machining steps of the milling process according to the procedure described in Section 3.3. The productivity analysis described in Section 3.4 is then performed for each of these segments. Once a segment has been analysed, the productivity data and segment boundaries are stored in the Influx database. The next step uses a Machine Learning (ML) model to analyse the data. New segments are continuously searched for in the Influx database and then analysed. Machining parameters such as feed  $f_z$ , cutting speed  $v_c$ , cutting width  $a_e$ , and cutting depth  $a_p$  as well as the tool angles  $\varphi_1$  and  $\varphi_2$  are determined from the measurement data. This requires further information about the product, such as the tools used and the dimensions of the blank. These data are retrieved from the corresponding product's asset administration shell (AAS). The information about the product must first be stored in the AAS. For this purpose, the Product Generator application has been developed. Using a random forest model from [7], the machine's energy consumption is predicted based on the measured data and the determined machine parameters. Furthermore, this work uses particle swarm optimization to determine the optimal parameters for each segment for the lowest possible energy consumption and tool wear and the highest possible surface quality. After the analysis, the determined data are also stored in the Influx database.

### 3.1. BaSyX Management Shell

The BaSyX management shell enables the unified description of digital twins. In the context of the framework, the management shell fulfils several tasks: On the one hand, the digital twin of the product to be manufactured provides the AI model with additionally required meta-information. On the other hand, current measurement data of the machine and characteristic values describing the machine state are represented in the machine's digital twin.

First, a digital twin of the product to be manufactured must be created. This consists of two submodels: the geometry submodel and the process submodel. The geometry submodel contains the dimensions of the blank and the material used as properties. On the other hand, the process submodel consists of a SubmodelElementCollection in which each tool is stored as a separate submodel. The submodel of a tool consists of the following properties: cutter diameter, cutter length, and number of teeth.



Conversely, the machine data should also be available in the management shell. This is made possible by the specially created management shell service. It establishes the connection between the Influx database and the AAS server, as seen in Figure 2. Each axis of the machine is represented by its submodel. Furthermore, there is a submodel describing the machine state. The current values of the various properties are retrieved directly from the Influx database using an automatic query.

### 3.2. ML Model

The created ML model is part of the cloud environment and analyzes the received data. It forms the main component of the framework, as seen in Figure 2. At the beginning, all timestamps of the segment boundaries from the last 5 min are queried from the Influx database. Then, a DataFrame is created that contains all calculated quantities of the segment that are needed for the energy prediction described in Section 2.3 as well as for the fuzzy system in Section 4.4.

For this purpose, the cutting depth  $a_p$ , the cutting width  $a_e$ , and the entry  $\varphi_1$  and exit angles  $\varphi_2$  of the tool are first determined according to the procedure described in Section 4.1. From the measured data of the machine, the tooth feed and the cutting speed are determined with knowledge of the tool data, which are retrieved from the management shell. A comparison with the productivity data ensures that the tooth feed and cutting speed assume zero value in unproductive areas since no material removal occurs here. Based on these variables, the metal removal rate is calculated for each productive time step of the segment. Furthermore, the current tool wear and surface quality are determined using the models described in Section 4.2. Through the procedure presented in [7], a modelling of the process forces for each of the three axes is performed.

The last step is predicting the current for each axis with the models presented in [7]. Therefore, a data frame with the input variables for the model is created. Since this requires values from the past and future, the current prediction is always delayed by one segment since the values from the future are only available with the new segment. In the same way, the values from the past are retrieved from the data frame of the previous segment. The determined time series with the predicted current values are transmitted to the Influx database. New segments are identified using the time stamp of the last segment from the previous query, so no segment is analysed twice. The values determined are then used to calculate relevant parameters, which are explained in more detail in Section 4.1. A fuzzy system finally evaluates these parameters, which generates recommendations to improve the machine state.

### 3.3. Segmentation

For segmentation, the subdivision based on the machining steps of the machine proves to be useful. These steps are defined in the NC code. However, the NC code is not always available in manufacturing. For this reason, these individual steps must be differentiated based on the recorded measurement data.

The basic procedure for segmenting the measurement data is explained in Figure 3. For the segmentation, the axis position of all three lines are relevant. A new machining step leads to an abrupt change in the nominal position of at least one of the three axes. The machining steps can be delimited based on these discontinuities. An exemplary course for the three axis target positions is shown in Figure 4. The measuring range of 20,000 data points corresponds to a period of 40 s. Here, several segments can be distinguished from each other. However, the discontinuities in the position course do not necessarily have to occur in all axes, as seen in Figure 4.

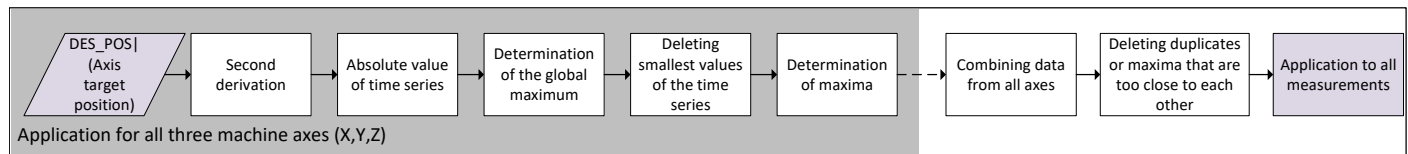


**Figure 3.** Schematic flow of the segmentation algorithm.

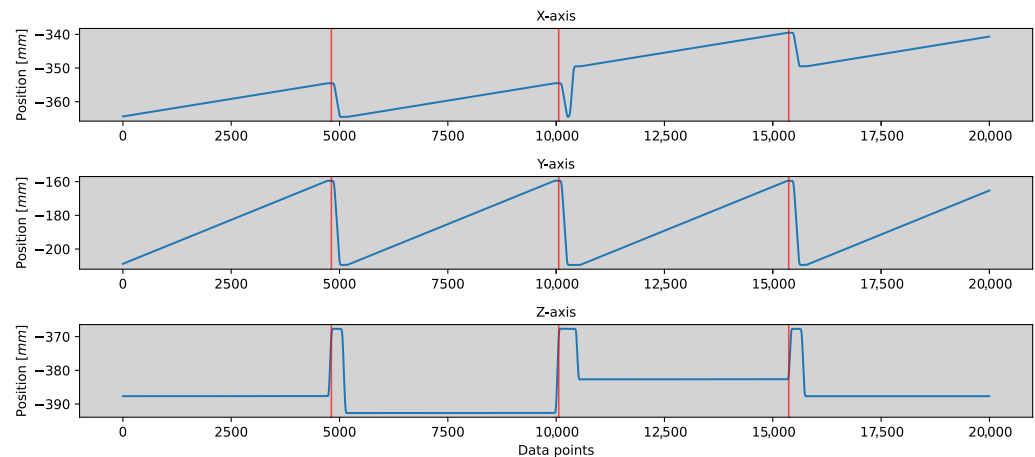


**Figure 4.** Exemplary segmentation for each axis using the target position.

A jump in the position course leads to very high values of the second time derivative, corresponding to the acceleration. In the next step, the local maxima of the acceleration must be identified. They define the boundaries between the individual segments. It should be noted that several extremes are often close to each other at a segment boundary, which can be maxima or minima. Therefore, the absolute value of the time series is used for the analysis to avoid distinguishing between positive and negative acceleration values. There are often smaller local extremes in the neighbourhood. This results in the need to preprocess the time series and filter the local maxima. In the first step, each of the three axes is analysed individually. Afterwards, the maxima found are assembled into a global solution.

Afterwards, the absolute value of the time series is calculated; thus, in subsequent steps, it is no longer necessary to distinguish between minima and maxima. Subsequently, the local maxima of the time series are determined. For each maximum, the position on the X-axis is stored. In the next step, the X-coordinates of the maxima of all three axes are combined so that the separation point is at the same position in each axis. The last step assigns these global separation points to all measured variables. Figure 4 illustrates this for the exemplary measured values of the three axes.

### 3.4. Productivity Determination

A procedure was developed to evaluate each segment's productivity, which will be explained in the following. The spindle energy and the spindle speed prove to be useful variables. The basic procedure of the productivity analysis is shown schematically in Figure 5. In the following, four different cases will be considered in which the segment or a part of the segment is classified as unproductive:

1. The velocities of the X and Y axes are both zero over the entire segment.
2. The spindle speed is zero.
3. The spindle speed is increased or decreased.
4. The spindle has reached setpoint speed but has not yet fully penetrated the material.

In reality, there is often a combination of these four cases. Figure 5 shows the procedure to determine the productivity of the segment. First, the velocities of the X and Y axes are considered. The tool does not change its position if these are zero over the entire segment. Consequently, the entire segment is classified as unproductive.

In the next step, the spindle power is considered. Before the spindle reaches zero speed, it usually decelerates from a higher speed. In consequence, the parts of the segment are classified as unproductive, as stated in Figure 5. Similarly, parts of the segment in which the spindle speed has the value zero are classified as unproductive as well.

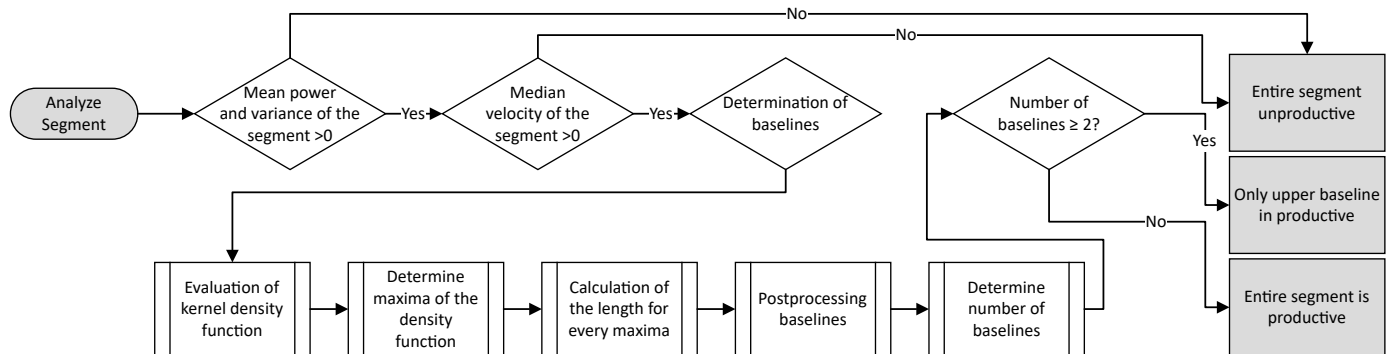


**Figure 5.** Schematic procedure for determining the productivity of a segment.

Next, we will consider the case in which the tool enters or exits the material. The spindle speed remains constant over the entire segment, but an increase in spindle power is visible when the tool enters the material. Accordingly, there is a drop in spindle power when the tool exits the material.

This course is exemplified in Figure 6a. A closer look at the electrical power shows that two levels can be distinguished. Outside the material, the power stays at a constant value at a constant speed. Similarly, the power value stays constant when the tool fully engages with the material. Consequently, for productivity analysis, the power value of these levels on the Y-axis and their length must be identified. This procedure will be explained in the following.

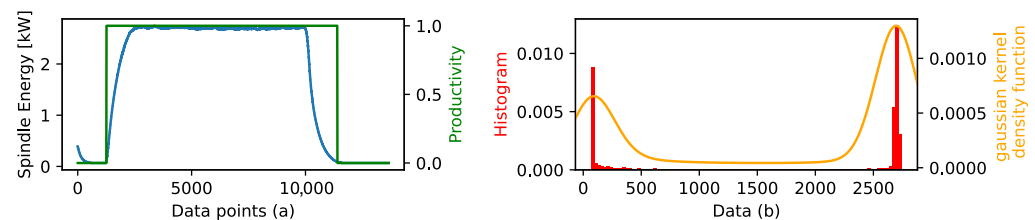


**Figure 6.** Example time series and its histogram.

In this case, these two values are identified by employing a kernel density function. Figure 6b shows the histogram and the KDF of the time series described at the beginning. Here, two maxima can be recognized. These represent the two energy levels of the time series. It was checked whether the values around the corresponding maxima were normally distributed. For this purpose, a Shapiro–Wilk test for normal distribution was performed. This yielded a  $p$ -value of  $p = 5.39 \times 10^{-39}$ . As a result, the data points cannot be assumed to be normally distributed.

The histogram approximation with the Gaussian KDF is, thus, subject to errors due to the lack of normal data distribution. This leads to a reduced accuracy of the determined values. This results in the necessity of locally post-processing the determined values. For this purpose, a sufficiently large search range must first be defined. This is selected according to the following formula:

$$\Delta y = 0.05 \times (1.1 \times P_{0.95}(ZR) - 0.9 \times \min(ZR)) \quad (1)$$

The frequency for each interval is determined in the range  $[y - \Delta y, y + \Delta y]$ . The value of the interval with the highest frequency is then used as the new value. In the next step,



the lengths of the energy levels are determined. This is achieved through summing up the number of data points whose energy values match the previously determined values of an energy level. However, not all data points lie precisely on this energy level, so it is essential to define a tolerance range. Following the standard deviation, a  $3 \times R$  value is chosen as the tolerance range. Thus, all values inside the range  $[y - 3 \times R, y + 3 \times R]$  are assigned to the energy level.

A minimum length prevents the results from being distorted by areas of constant energy with a short length. On the other hand, all areas that are not at the lower level are classified as productive. Applying this procedure to the time series in Figure 6a results in the productivity classification shown in Figure 7a. It is noticeable that at the beginning of the time series, one area was incorrectly classified as productive because the data points were outside the tolerance range of the energy level. This results in the necessity of post-processing. It is assumed that no productive areas can occur at the edges if an unproductive area follows shortly after. Therefore, unproductive regions, in this case, are extended to the left and right edges, respectively, as shown in Figure 7b.

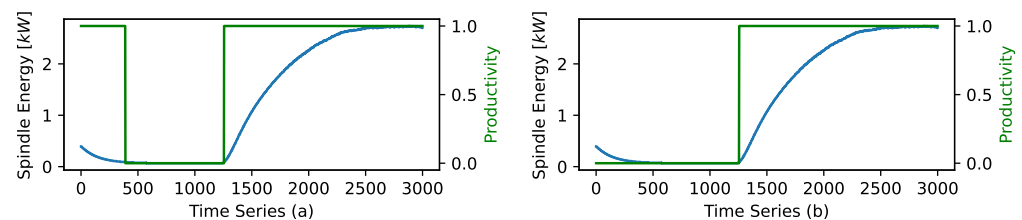


**Figure 7.** Productivity of the example time series. Left without extension to the edge, right with extension to the edge.

## 4. Implementation

### 4.1. Determination of Milling Parameters

#### 4.1.1. Retrieving Product Data from the Management Shell

For calculating the tool diameter  $D$  milling parameters, the number of teeth  $z$  and the tool length  $l$  are relevant. The recorded position data enable the recognition of a tool change. In this case, the following tool is retrieved from the tool list, and the tool information is updated accordingly. Furthermore, the material used for the part is retrieved from the AAS.

#### 4.1.2. Determination of the Cutting Width

Determining the cutting width  $a_e$  is based on analysing previous machining steps. It is assumed that the part is machined in parallel paths. Consequently, two adjacent parallel toolpaths are offset from each other. Thus, to determine  $a_e$ , the closest path must be identified from past measurement data.

The parallel paths can be identified by comparing the current segment with all previous segments of the measurement data. If two paths are parallel, their distance in the XY plane is constant over the entire length. For this purpose, each of the two segments is subdivided into 150 grid points. Then, for each grid point, the distance to the 150 grid points of the comparison segment is calculated using the Euclidean distance. The point with the smallest distance is then the closest. This procedure is shown in as an example for four grid points in Figure 8. From this, it is clear that for a parallel segment, the distance must be identical for all 150 grid points. For a non-parallel segment, however, this distance is not constant.

In the last step, the minimum distance is determined by comparing all previous segments corresponding to the cutting width.

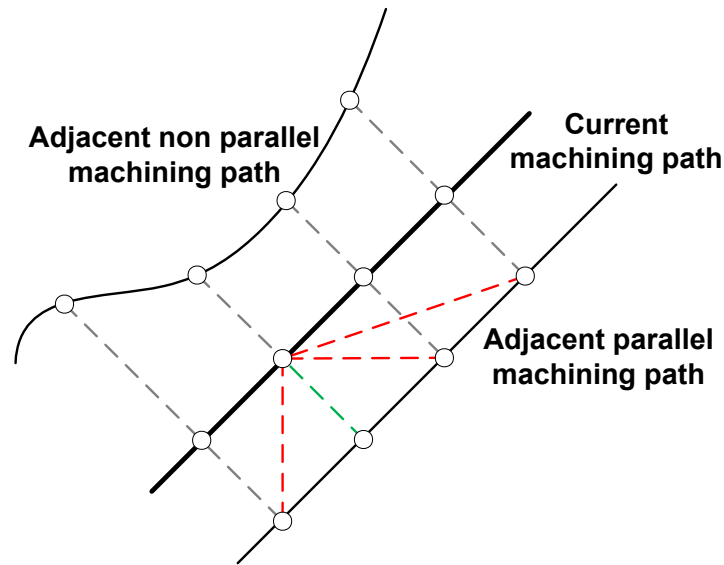


**Figure 8.** Determination of the cutting width.

#### 4.1.3. Determination of Tool Angles

The entry angle  $\varphi_1$  and the exit angle  $\varphi_2$  are essential for calculating the forces during machining. To determine these, in addition to the cutting width  $a_e$ , it is also required to know whether the tool enters the material with the left or right side. For this purpose, a reference point on the toolpath of the segment in the XY plane is considered. In the next step, the distance to the nearest parallel path is determined for this reference point ( $X_{Ref}, Y_{Ref}$ ).

For each point on the neighbouring path, the Euclidean distance is calculated. The point with the smallest distance is, thus, the closest point on the neighbouring path. For these two points, the distance  $\Delta X = X_{current} - X_{previous trajectory}$  in the X direction and analogously  $\Delta Y$  in the Y direction are determined using the Euclidean distance. The next step is to consider the velocities  $v_x$  and  $v_y$  of the tool on the current path in the X and Y directions. Different cases can be distinguished by determining the position of the paths to each other when considering the distances and velocities in the X and Y directions. In the case of a horizontal path, for example, the material to be machined is located to the left of the cutting edge if  $V_x > 0$  and  $\Delta_y > 0$ . Analogously, other cases can be distinguished, as seen in Figure 9.

Based on this information and utilizing the cutting width  $a_e$ , the tool's entry angle  $\varphi_1$  and the exit angle  $\varphi_2$  can finally be determined, knowing the tool diameter  $D$ . If the material is located to the left of the cutting edge, the entry angle  $\varphi_1 = 0^\circ$  and the exit angle is calculated according to the following formula:

$$\varphi_2 = \arcsin\left(\frac{R - a_e}{R}\right) \times \frac{180^\circ}{\pi} + 90^\circ \quad (2)$$

The material to be machined is located to the right of the cutting edge, the following relationship applies to the entry angle:

$$\varphi_1 = \arccos\left(\frac{R - a_e}{R}\right) \times \frac{180^\circ}{\pi} \quad (3)$$

Through these constraints the exit angle has the value  $\varphi_2 = 180^\circ$ .

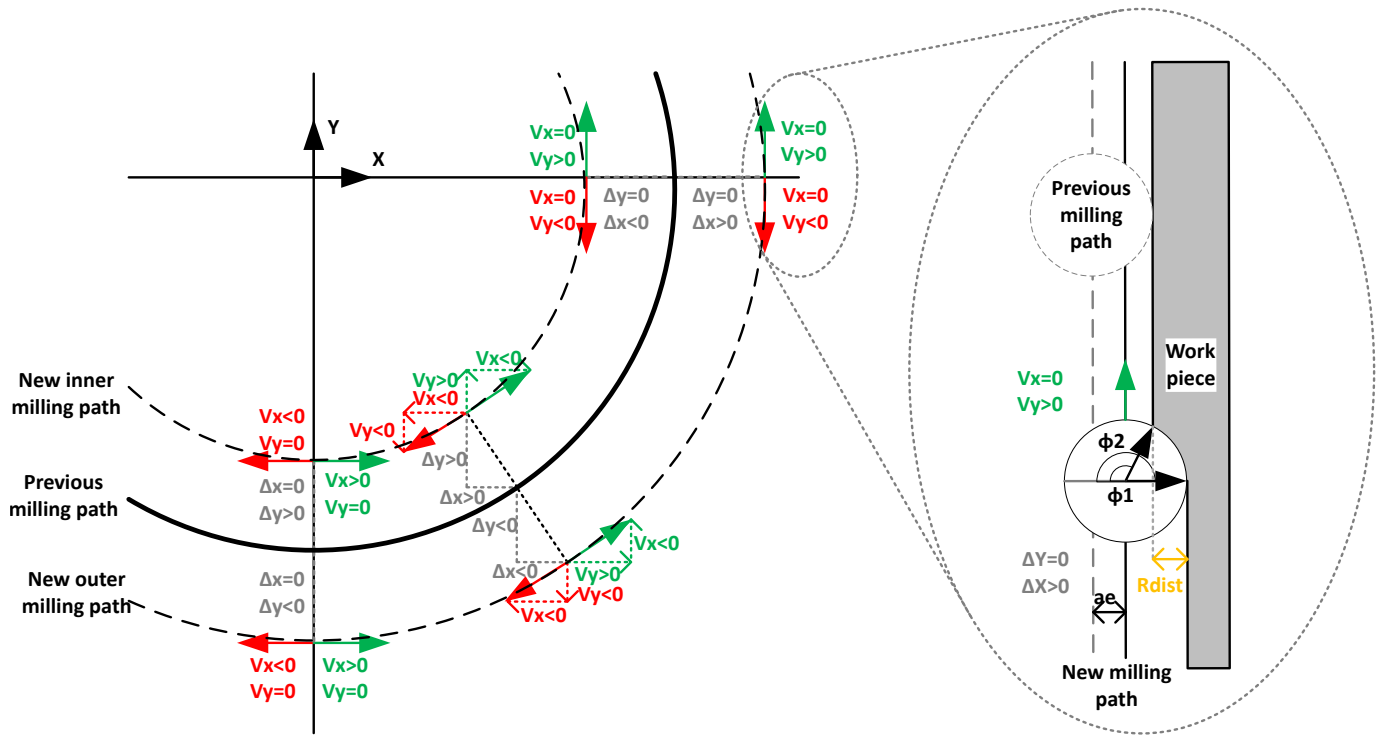


Figure 9. Determination of material position and tool angles.

#### 4.1.4. Determination of the Cutting Depth

Based on the information from the AAS, the cutting depth  $a_p$  for the uppermost toolpath can be calculated using the position data. After the cutter has removed the workpiece's first layer, the subsequent layer's cutting depth can be determined using the previous measurement data. The prerequisite for this is that the paths lie precisely on each other. In this case, the cutting depth can be determined by the following procedure.

In the first step, segments must be determined from the previous measurement data with the same path in the XY plane as the current segment. For this purpose, a histogram is created from the position data in the X and Y directions of the current path and the path from the comparison segment. In the next step, another histogram is created from both histograms, in which the classes with the same value are subtracted. The absolute value of this difference gives the value of the new histogram for the corresponding class. The classification, whether the trajectory of two segments is identical, will be shown in the following with exemplary segments.

In Figure 10, the position data of two segments are compared. On the left side of the figure, two segments with different trajectories are shown (segments 1 and 2). When looking at the difference, it becomes clear that the histograms of segments 1 and 2 differ strongly, especially in the marginal area. The two segments, 3 and 4, describe the same path. Looking at the difference, it becomes clear that the two histograms have only minor differences. For this evaluation, the sum of the frequencies is calculated as the integral for each of the three histograms described. Finally, the ratio of the integral of the different histograms is calculated according to Formula (4).

$$\Delta Hist = 1 - \frac{Hist_{Differenz}}{Hist_1 - Hist_2} \quad (4)$$

Two paths are classified as identical from a value of  $\Delta Hist > 0.7$ . Finally, the depth of cut can be determined by the difference in the Z-position of the two segments.

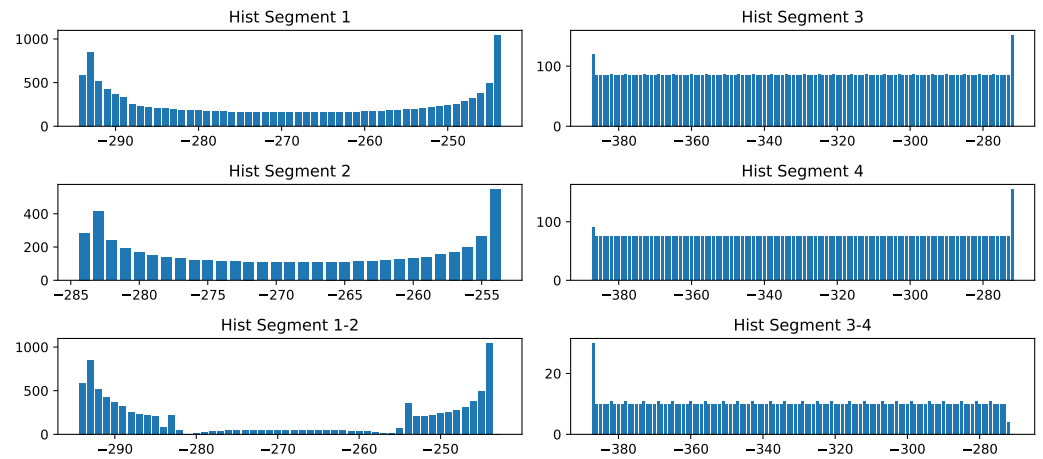


**Figure 10.** Comparison of histograms for different trajectories (**left**) and identical trajectories (**right**).

#### 4.1.5. Calculation of Further NC Parameters from the Measured Data

Further machine parameters must be determined for the segment under consideration for the subsequent parameters' calculation. The speed is calculated for each segment using the median of the recorded angular speed of the spindle:

$$n = VEL_{FFW,6} \times \frac{60s}{360^\circ} \quad (5)$$

The tool diameter  $D$  is retrieved from the management shell, the cutting speed  $v_c$  can be calculated from the rotational speed according to (6).

$$v_c = \frac{n \times \pi \times D}{\text{mm/m}} \quad (6)$$

For calculating the tooth feed  $f_z$ , the velocity in the XY plane is calculated by vector addition of the velocity components  $v_X$  in the X direction and  $v_Y$  the Y direction:  $v_{XY} = \sqrt{v_X^2 + v_Y^2}$ .

This calculation is performed for each measuring point of the time series. Only afterwards is the median formed from all measuring points. Finally, knowing the tool diameter  $D$  and the number of teeth  $z$ , the tooth feed  $f_z$  is calculated according to Equation (7).

$$f_z = \frac{v_f}{z \times n} \quad (7)$$

During machining, a tool change must also be detected. In the case of a tool change, the spindle moves to a particular tool change position ( $z = 0$ ). In this case, the data from the following tool are used.

#### 4.2. Optimization Models

When optimizing the machine parameters, the aim is to achieve the best possible surface quality while achieving a high material removal rate, low energy consumption, and low tool wear. For this purpose, models are developed, which can be used to optimize the NC parameters considered in this work: cutting depth  $a_p$ , cutting velocity  $v_c$ , and tooth feed  $f_z$ .

##### 4.2.1. Surface Quality

A decision tree combines the models for an enlarged parameter space based on the regression models presented in Section 2.1. In doing so, the range of values considered for the input variables is first determined for each regression model. Subsequently, the boundaries between the parameter spaces of the individual models are determined. The

models are distinguished between steel and aluminium. The models are changed based on the values of the input variables. Finally, a limit is defined for each of the three variables, which they must not exceed. The maximum cutting depth  $a_p$  is 2.5 mm for aluminium and 1.5 mm for steel. The tooth feed  $f_z$  must not exceed 0.25 mm/rev in both cases. Similarly, the cutting speed  $v_c$  must not exceed 150 m/min. All relevant rules for switching between the individual models are visualized as a decision tree in Figure 11. The regression model presented in the corresponding paper is then used to calculate the surface quality.

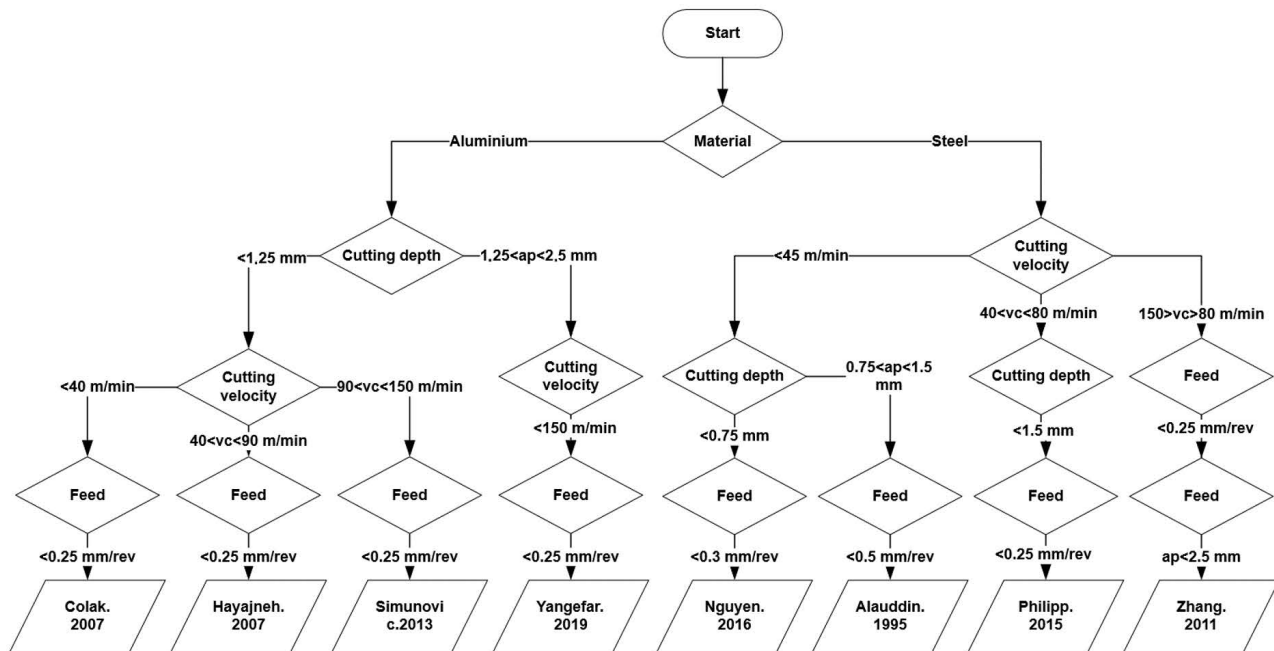


Figure 11. Decision tree to determine the appropriate regression model [9–16].

#### 4.2.2. Energy Consumption

The energy consumption is determined based on the model of [7] described in Section 2.3. Since the voxel simulation is not suitable for real-time analysis due to its long computation time, it has to be replaced. Instead, the relevant quantities are extracted directly from the measured data. First, the input variables  $a_c$ ,  $a_p$ ,  $\varphi_1$ , and  $\varphi_2$  and the material removal rate relevant to the neural network are calculated. In addition to these quantities, the tooth feed rate  $f_z$  and the cutting speed  $v_c$  are determined. This information calculates the forces for all axes using Kienzle's cutting force formula. These variables form the input variables for the random forest model, which is then used to predict the current values. In addition to predicting the current power consumption, the energy consumption model performs another task. For the particle swarm optimization function in Section 4.2.5, it is necessary to predict the current value for different values of  $a_p$ ,  $f_z$ , and  $v_c$ . The optimization with the particle swarm is performed for each segment. Therefore, segment data are combined with these free parameters. First, assumptions have to be made about this. It is assumed that the processing is in the XY plane. Consequently, the velocity in the Z direction  $v_z$  is zero. Furthermore, it is assumed that the velocity is constant, and consequently, the acceleration in all axes has zero value. The tool angles  $\varphi_1$  and  $\varphi_2$  are taken from the real segment. The direction of machining in the XY plane is kept, but the speeds are adjusted to correspond to the feed ( $f = \sqrt{v_x^2 + v_y^2}$ ). The cutting speed again determines the spindle speed. However, since the model has been trained to predict time series, it is not possible to predict individual time points with the model. For this reason, the force values are considered instead of the current values. These force values were determined using the Kienzle cutting force formula, as explained in more detail in [7]. Figure 12 shows the sum of the measured current values from all four axes of the milling machine and the

sum of the calculated forces from all four axes. The reason for values above 10 kN comes from the cumulated sum of forces for the feed axis and the spindle, which normally cancel each other out to a certain point. The current is the sum of all individual currents for the four axes. This necessitates looking at the sum of all force components, which are, in some cases, actio and corresponding reactio forces because the motor has to deliver the necessary torque. This figure should illustrate that there is a qualitatively similar progression of the two variables that can be recognized. Accordingly, using the force values instead of the energy for the optimization function is acceptable for a first proof of concept.

After the optimization model has determined the optimum NC machining parameters, the energy is calculated again using these parameters. This makes it possible to determine the possible savings in energy consumption. Since the machining time changes when the feed rate changes, the individual segments' energy consumption is scaled to enable comparability. The optimized energy is first determined using the new NC parameters. The energy is then scaled by Formula (8).

$$E_{opt_{skaliert}} = E_{opt} \times \frac{a_p}{a_{p,opt}} \times \frac{f_z}{f_{z,opt}} \quad (8)$$

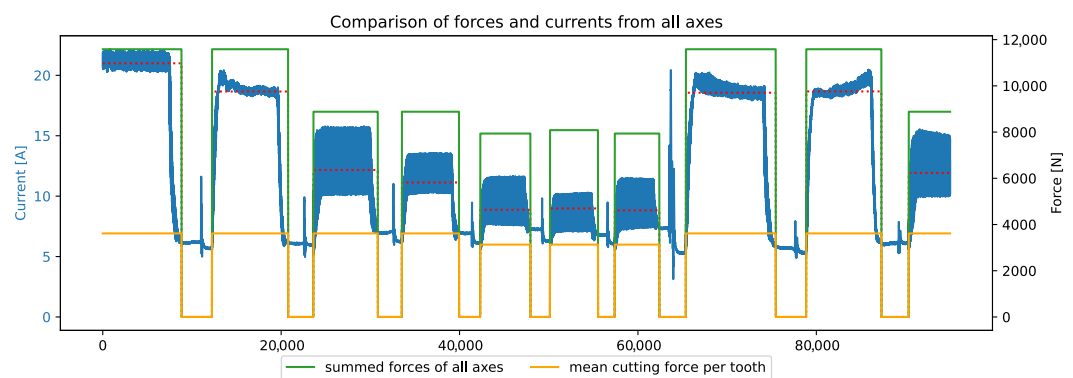


**Figure 12.** Actual current values (with median in red) and calculated forces summed over all four axes.

#### 4.2.3. Tool Wear

Tool wear is determined using the regression model of [17] explained in Section 2.2. Since this model covers a large parameter space, switching between multiple models is unnecessary, as applied in Section 4.2.1 for surface quality.

#### 4.2.4. Setting Up an Optimization Function

The optimization function combines tool wear, surface quality, energy consumption, and material removal rate variables. The energy consumption is replaced by the calculated forces as a substitute, as explained in Section 4.2.2. Since the optimization variables have different ranges of values, it is necessary to scale them. For this purpose, the optimization variables are normalized according to Equation (9).

$$X_{Norm} = \frac{X - X_{Min}}{X_{Max} - X_{Min}} \quad (9)$$

Since the models for surface roughness and tool wear cover only cutting depths up to 1.5 mm, according to [15,23], a linear increase in these quantities is assumed for larger cutting depths. A linear correlation is assumed analogously for the tooth feed according to [15]. However, this depends on the regression model used since they have different maximum values for the tooth feed. Finally, the four optimization variables are combined in an optimization function. This is described by Equation (10) for steel as a material.

$$Y = 6.7 \times Ra_{Norm} + 6 \times TW_{Norm} - 11.48 \times MRR_{Norm} + 3 \times F_{Norm} \quad (10)$$



(11) is the optimization function for aluminium as a material.

$$Y = 6.7 \times Ra_{Norm} + 4.6 \times TW_{Norm} - 22.7 \times MRR_{Norm} + 4.6 \times F_{Norm} \quad (11)$$

High surface roughness values, tool wear, and process forces worsen the value of the optimization function. However, since low values for cutting speed, tooth feed, and cutting depth are preferred, the material removal rate is also used as a penalty term. A high material removal rate thus reduces the value of the optimization function. The weights for the various terms of the optimization functions in (10) and (11) are determined by varying the weights so that the function converges towards an optimum that does not lie in the marginal regions.

#### 4.2.5. Particle Swarm Optimization

For the optimization functions described in Section 4.2.4, the optimal values of the complimentary input parameters ( $a_p$ ,  $f_z$ ,  $v_c$ ) are determined by particle swarm optimization. The population consists of 800 particles. The values  $c_1 = 1.5$  and  $c_2 = 0.65$  are chosen as the social and cognitive weighting factors, respectively. For inertia, the value  $\beta = 0.3$  is used. The edges are defined as a fixed boundary, meaning the particles are absorbed.

#### 4.3. Calculation of Parameters

Based on the values determined by the AI model, parameters for evaluating the machining conditions are evaluated in the next step. All parameters are calculated for five minutes. Table 2 shows the different parameters and their description. For some parameters, a comparison is made between the values determined by the optimization model and those occurring in reality for various optimization parameters. These deviations make it possible to estimate the optimization potential of the machine.

**Table 2.** Machine condition assessment parameters.

| Code                            | Description   |
|---------------------------------|---|
| Productivity<br>Energy per path | Share of total productive energy<br>Total energy divided by path  |
| Deviation spindle current       | Mean value of the difference between measured spindle current and predicted spindle current in the considered period                                    |
| Deviation energy consumption    | Deviation between the energy consumption predicted with the current NC parameters and the energy consumption predicted with the optimized NC parameters |
| Surface quality                 | Mean value of the surface quality calculated for the actual machine parameters with the model in the considered period                                  |
| Difference surface quality      | Difference between the optimized and actual surface quality   |
| Tool wear                       | Mean value of tool wear calculated for the actual machine parameters with the model in the considered period  |
| Material removal rate           | Removed material volume in the last 5 min   |

#### 4.4. Fuzzy System

The fuzzy system is part of the AI model described in Section 3.2. Based on the parameters explained in Table 2, the fuzzy system calculates the degree of fulfilment of the various recommendations. For this purpose, suitable recommendations are first formulated, which are listed below:

- “By using the optimized milling parameters, the surface quality could be improved”.
- “The tool wear could be reduced by using the optimized milling parameters”.
- “The milling conditions are [Good / Average / Bad]”.
- “Attention! The spindle current is higher than expected”.
- “By using the optimized milling parameters, the energy consumption could be reduced”.
- “Optimizing the NC program can improve productivity”.

- (g) “The metal removal rate seems to be [low / very low]; by choosing the optimized parameters, it can be improved”.

The recommendations are linked to the parameters explained in Section 4.3 in the next step. Here, suitable parameters are identified for each recommendation. Table 3 shows the linkage between them. In the next step, the input variables and the output variable are described by fuzzy membership functions. Subsequently, these are linked by a suitable rule base, which is finally used to determine the output variable, in this case, the degree of fulfilment of the corresponding recommendations.

**Table 3.** Linking recommendations and key performance indicators.

| Indicator                    | Recommendation |     |     |     |     |     |     |
|------------------------------|----------------|-----|-----|-----|-----|-----|-----|
|                              | (a)            | (b) | (c) | (d) | (e) | (f) | (g) |
| Productivity                 |                |     |     |     |     |     |     |
| Energy per way               |                |     |     |     |     |     |     |
| Deviation spindle current    |                |     |     |     |     |     |     |
| Deviation energy consumption |                |     |     |     |     |     |     |
| Surface quality              |                |     |     |     |     |     |     |
| Difference surface quality   |                |     |     |     |     |     |     |
| Tool wear                    |                |     |     |     |     |     |     |
| Difference tool wear         |                |     |     |     |     |     |     |
| Machining volume             |                |     |     |     |     |     |     |

#### 4.4.1. Fuzzification of Input and Output Variables

First, the input variables are described fuzzily by membership functions. Standard partitions give the description of the membership functions. The membership functions map individual linguistic terms. The partitioning of productivity is performed by the three linguistic terms “poor”, “average”, and “good”. Furthermore, this partition is not necessarily equidistant. The choice of cut points and their concrete scalar values is based on training data and expert knowledge. Analogously, the output variable is also described by linguistic terms. The corresponding recommendation is only issued when the output variable exceeds a certain limit value. Finally, the corresponding membership functions are determined for concrete values of the input variables.

#### 4.4.2. Establishing and Evaluating a Rule Base

The rule base describes rules linking input variables with output variables. In this case, it is a Mamdani fuzzy system. Many rules are required to consider all combinations of the possible values of the input variables. In Table 4, all rules for determining the machine state are listed. A separate rule base is defined for each output variable using the same procedure based on its input variables.

**Table 4.** Fuzzy rule base for machine state determination.

| Cutting Volume: Low |           | Cutting Volume: Large |          |                 |           |        |          |
|---------------------|-----------|-----------------------|----------|-----------------|-----------|--------|----------|
| Energy per path     | Low       | Medium                | High     | Energy per path | Low       | Medium | High     |
| Productivity        |           |                       |          | Productivity    |           |        |          |
| Poor                | Bad       | Very bad              | Very bad | Poor            | Medium    | Bad    | Very bad |
| Average             | Medium    | Medium                | Poor     | Average         | Good      | Good   | Medium   |
| Good                | Very good | Good                  | Medium   | Good            | Very good | Good   |          |

The definition of the rules is based on expert knowledge. The premise evaluation determines the degree of fulfilment for each of these rules. The minimum operator links

the AND condition. Here, the minimum of all affiliations of the input variables is chosen as the degree of fulfilment of the corresponding rule. Often, several rules have the same conclusion. Through an AND operation, each linguistic term has a membership value independent of the individual rules. This step is also called accumulation.

In the following step, the scalar value for the corresponding output variable is calculated using the centroid method. After the output variables for all recommendations have been calculated, a decision is made based on previously defined limit values on whether the corresponding recommendation is applicable. The choice of these limit values is based on the membership functions. For some recommendations, the membership value itself is also part of these. For example, the machine state is characterized by the corresponding membership value.

## 5. Validation

The developed framework was tested using the parts described in Section 2.5. In the following, only the results with steel as material are considered, as these differ only slightly from those with aluminium.

The segmentation mainly worked well for the training part. The individual machining steps of the NC program were recognized. Still, some machining steps were partially divided into segments, as shown in Figure 13 approximately at 14,000 and 20,000 data points. The segments were classified correctly in the productivity determination, but the classification worked better in the first half of the machining. In the second half, the individual areas within a segment cannot always be distinguished. A comparison between the measured and the predicted spindle current by the random forest model shows only minor deviations. On the other hand, the power consumption is only a fourth when using the optimized parameters. However, tool wear increases when using the optimized parameters from Figure 14. The surface quality also deteriorates by a factor of 1.5–3. The AAS provides information about the tools' properties, such as the tool diameter  $D$ , as described in Section 3.1. A corresponding process submodel was previously defined for the part. Conversely, the tool change is automatically recognized in the measurement data using the procedure described in Section 4.1.5. The current cutting depth for this part was correctly determined to be a constant 10 mm in the first half and a constant 5 mm in the second half. The optimization model recommends a reduction in the cutting depth to 3–4 mm. In contrast, a strong increase of 0.1 or 0.05 mm/rev to the maximum value of 0.5 mm/rev is recommended for the tooth feed. There were two tool changes on this part. These were correctly detected in the measurement data.

The recommendations recommend an adjustment of the NC parameters to reduce energy consumption. Furthermore, the fuzzy system identifies the potential for productivity improvement. However, this assessment cannot be confirmed when looking at the productive shares in Figure 15.

The segments were also reliably detected by analysing the validation part. The productivity of the segments was classified correctly, but within a segment, the individual areas could not always be clearly distinguished from one another. A comparison between the measured and predicted spindle current using the random forest model showed large deviations in some cases. The predicted current is four times as large as the current requirement. On the other hand, the current requirement is four times smaller when the optimized parameters are used compared to the actual calculated current requirement. When using the optimized parameters from Figure 16, tool wear increases in some cases. The surface quality deteriorates by a factor of 2–3. On the other hand, a strong increase from 0.05 mm/rev to the maximum value of 0.5 mm/rev is recommended for the tooth feed. However, these feed rates cannot be realized for the tool diameters (10 mm to 20 mm).

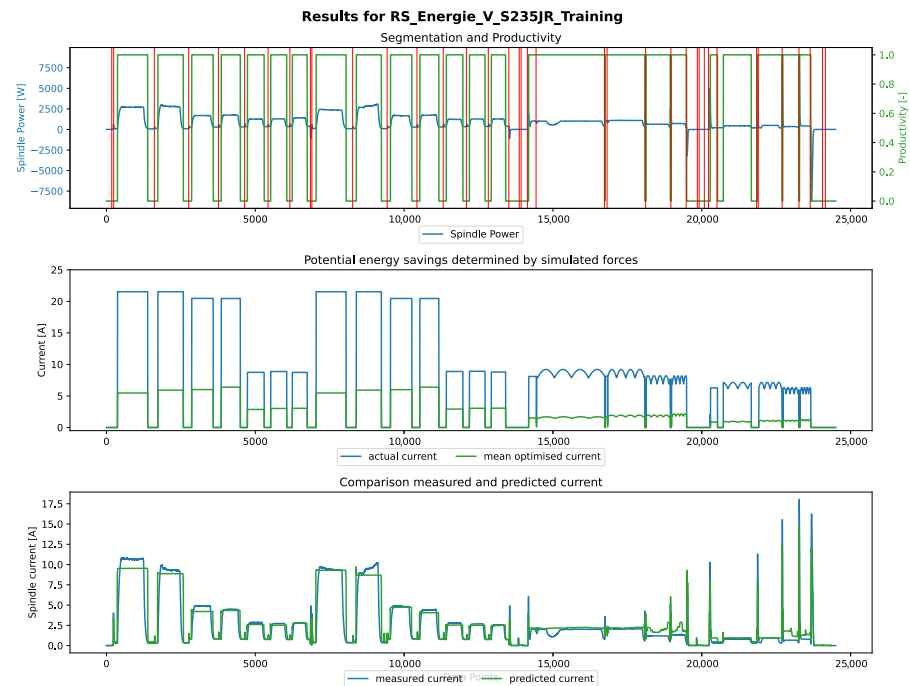


**Figure 13.** Result of segmentation and productivity determination as well as optimal and predicted power consumption for the training part (steel).

->The machine condition is satisfactory

->By using the optimized milling parameters, the energy consumption could be reduced

->Optimized NC parameters: Feed rate: 0.5 mm/rev, cutting speed: 122.385 m/min, Cutting depth 3.257 mm

->By optimizing the NC program, productivity can be improved

->The surface quality is: 0.0% poor, 57.13% average, 42.87% good

->The tool wear is: 70.18% low, 29.82% medium, 0.0% high

**Figure 14.** Generated recommended actions for the training part with material steel.

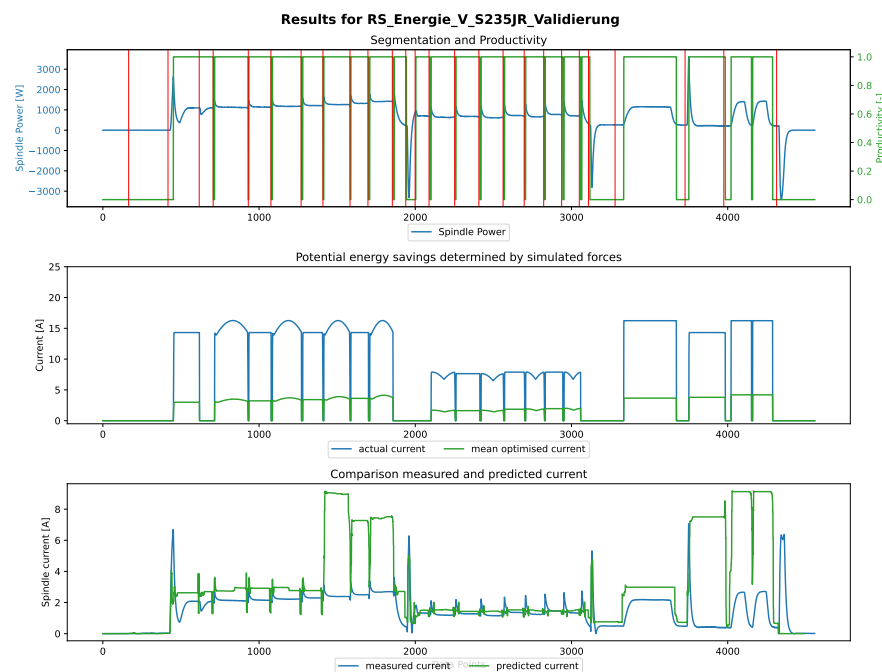


**Figure 15.** Result of segmentation and productivity determination as well as optimal and predicted power consumption for the validation part (steel).

->The machine condition is satisfactory  
 ->By using the optimized milling parameters, the energy consumption could be reduced  
 ->Optimized NC parameters: Feed rate: 0.5 mm/rev, cutting speed: 122.459 m/min, Cutting depth 2.672 mm  
 ->By optimizing the NC program, productivity can be improved  
 ->The surface quality is: 0.0% poor, 51.72% average, 48.28% good  
 ->The tool wear is: 79.68% low, 20.32% medium, 0.0% high

**Figure 16.** Generated recommended actions for the validation part with material steel.

The fuzzy system correctly identifies potential savings in energy consumption when using the optimized NC parameters. Particularly in the second half of machining, the individual segments sometimes have more significant unproductive portions. Correctly, the fuzzy system identifies this circumstance and recommends optimization of the NC program to improve productivity.

## 6. Evaluation

When validating with real measurement data, the chosen approach reliably divides the data into individual segments corresponding to the NC steps. Subsequently, the productivity of the individual segments could be determined. By comparing the individual segments, the various NC parameters, such as the cutting depth, the cutting width, and the tool angles, could then be determined from the measurement data. Additional information, for example, about the tools used, could be retrieved from an asset administration shell. However, there are still limitations. For example, the cutting depth can only be determined if two segments in the XY plane have the same path.

Due to the modular structure of the framework, it is possible to integrate existing models. This was demonstrated using the previously developed energy prediction model of [7]. An optimization model was developed in Section 4.2, combining the three variables of tool wear, surface quality, and energy consumption to determine the optimal NC parameters. However, the model for estimating surface quality only makes a general statement. To improve the prediction quality, it would make sense to carry out tests directly on the milling machine for which the model is to be developed and to consider other influencing variables. A regression model also describes tool wear. This model also considers only a few influencing parameters and, therefore, only makes a very general statement. The energy consumption prediction is based on the work of [7]. In this work, the voxel ablation simulation of [7] was successfully replaced, and the input variables of the neural network were determined and calculated from the measurement data instead. This made it possible to use the model in real time. A function combines the different models, and then the optimal processing parameters are determined by particle swarm optimization. However, because of the very general models, only partially meaningful values could be determined for the NC parameters. The maximum feed rate of 0.5 mm/rev for steel parts was determined as the optimum value, as stated in Section 5. Such a high feed rate theoretically leads to a shorter processing time and, thus, to energy savings. However, in combination with a high cutting depth, this value is not feasible in reality, as temperatures would be too high during machining, and tool wear would increase massively. For this reason, it was not possible to validate the optimum values determined by the model. This limitation is due to the partially inaccurate surface quality and tool wear models, which are based on literature values. These models were only developed to analyse the individual target variables. In our holistic approach, these models are combined. As a result, unfavourable parameter values can be recommended when combining the models. Therefore, more precise models would have to be developed for real-world use in further investigations, considering the other target variables. Nevertheless, the framework's basic functionality could be demonstrated by applying it to various test parts. In Section 5, it was shown that a fuzzy system based on these parameters can describe the machine condition. Subsequently, recommendations for improving the machining condition were generated for various parts. In this case, the fuzzy system was used to

determine the degree of fulfilment of the corresponding recommendation. Looking at the recommendations generated in Section 5, it can be concluded that the chosen approach is suitable for identifying optimization potential in milling. The developed framework was tested based on four different parts. In the process, sensible recommendations were generated for all parts. The framework is, therefore, suitable for real-world use and can also be applied to unknown parts.

## 7. Summary and Outlook

Increasing the energy efficiency of milling machines is the subject of several research studies. More efficient manufacturing can reduce the manufacturing costs and CO<sub>2</sub> emissions of products. To make this possible, this work developed and implemented a framework for automatically analysing measurement data. This framework analyses the measurement data provided by the machine. The milling parameters are extracted from the measurement data for a reference implementation. Using an AI model, the parameters are then optimized, and indicators are calculated to describe the machining conditions. Based on these indicators, recommendations for improving the machining conditions are generated in the final step.

A fuzzy system was used to describe the machine state and generate recommendations to improve milling conditions. For validation, the implementation of the framework was tested with four different parts. The approach developed in this work can detect milling conditions during machining and generate recommendations for milling improvement in real time. However, more precise models for the different variables of the optimization model should be developed before this approach can be used in real applications. Moreover, the introduced segmentation steps underlie constraints in this stage to reduce the complexity and enable the investigation of the holistic concept.

The modular design of the framework makes it easily adaptable. The framework could also be used for machines like lathes or 3D printers. For this purpose, the models used can be easily exchanged and new parameters defined.

Future investigations could focus on the influence of part orientation. Ref. [7] investigated the influence of workspace orientation on the repeatability of robots. This approach could also be transferred to the milling machine considered in this work.

**Author Contributions:** Conceptualization, A.B. and R.S.; methodology, S.A.; software, S.A. and R.S.; validation, S.A. and R.S.; formal analysis, S.A. and A.B.; investigation, S.A., A.B., and R.S.; resources, J.F. and A.W.; data curation, S.A. and R.S.; writing—original draft preparation, S.A. and A.B.; writing—review and editing, S.A. and A.B.; visualization, S.A.; supervision, A.B. and J.F.; project administration, J.F. and A.W.; funding acquisition, J.F. and A.W. All authors have read and agreed to the published version of the manuscript.

**Funding:** This publication is based on the research results of the project “SDMFlex-Flexible SDM through Continuously Quality-aware Digital Twins”. The authors would like to thank the Ministry of Science, Research and Arts of the Federal State of Baden-Württemberg for the financial support of the projects within the InnovationCampus Future Mobility (ICM).

**Data Availability Statement:** The data presented in this study are openly available in KITopen Repository at DOI: 10.5445/IR/1000157789, reference number KITopen-ID: 1000157789.

**Conflicts of Interest:** The authors declare that they have no known competing financial interests or personal relationships that could have appeared to influence the work reported in this paper.



## Abbreviations

| Name                      | Symbol      | Unit                            |
|---------------------------|-------------|---------------------------------|
| Feed Rate                 | $v_f$       | mm/min                          |
| Cutting Speed             | $v_c$       | m/min                           |
| Width of Cut (Engagement) | $a_e$       | mm                              |
| Depth of Cut              | $a_p$       | mm                              |
| Tool Diameter             | $D$         | mm                              |
| Spindle Speed             | $n$         | -                               |
| Tooth Feed                | $f_z$       | mm/rev                          |
| Number of Teeth on Tool   | $z$         | -                               |
| Cutting Force             | $F$         | N                               |
| Active Force              | $F_a$       | N                               |
| Passive Force             | $F_p$       | N                               |
| Feed Direction Angle      | $\varphi$   | °                               |
| Feed Force                | $F_f$       | N                               |
| Feed Normal Force         | $F_{fn}$    | N                               |
| Specific Cutting Force    | $k_c$       | N/mm <sup>2</sup>               |
| Energy Consumption        | $E$         | W                               |
| Basic Energy Requirement  | $P_0$       | W                               |
| Material Removal Rate     | $\dot{v}$   | mm <sup>3</sup> s <sup>-1</sup> |
| Wear Mark Width           | $B$         | μm                              |
| Average Roughness         | $R_a$       | μm                              |
| Standard Deviation        | $\sigma$    | -                               |
| Entry Angle               | $\varphi_1$ | °                               |
| Exit Angle                | $\varphi_2$ | °                               |

## References

- Bhat, S. *Practical Docker with Python*; Apress: Berkeley, CA, USA, 2022. [CrossRef]
- BDEW. (15 February 2023) Industriestrompreise<sup>1</sup> (Inklusive Stromsteuer) in Deutschland in den Jahren 1998 bis 2023 (in Euro-Cent pro Kilowattstunde) [Graph]. Available online: <https://de.statista.com/statistik/daten/studie/252029/umfrage/industriestrompreise-inkl-stromsteuer-in-deutschland/> (accessed on 7 September 2023).
- Moradnashad, M.; Unver, H.O. Energy efficiency of machining operations: A review. *Proc. Inst. Mech. Eng. Part B J. Eng. Manuf.* **2017**, *231*, 1871–1889. [CrossRef]
- Shin, S.J.; Woo, J.; Rachuri, S. Energy efficiency of milling machining: Component modeling and online optimization of cutting parameters. *J. Clean. Prod.* **2017**, *161*, 12–29. [CrossRef]
- Tapoglou, N.; Mehnen, J.; Butans, J.; Morar, N.I. Online on-board Optimization of Cutting Parameter for Energy Efficient CNC Milling. *Procedia CIRP* **2016**, *40*, 384–389. [CrossRef]
- Tapoglou, N.; Mehnen, J.; Vlachou, A.; Doukas, M.; Milas, N.; Mourtzis, D. Cloud-Based Platform for Optimal Machining Parameter Selection Based on Function Blocks and Real-Time Monitoring. *J. Manuf. Sci. Eng.* **2015**, *137*, 040909. [CrossRef]
- Ströbel, R.; Probst, Y.; Deucker, S.; Fleischer, J. Time Series Prediction for Energy Consumption of Computer Numerical Control Axes Using Hybrid Machine Learning Models. *Machines* **2023**, *11*, 1015. [CrossRef]
- Maher, I.; Eltaib, M.E.H.; Sarhan, A.A.D.; El-Zahry, R.M. Investigation of the effect of machining parameters on the surface quality of machined brass (60/40) in CNC end milling—ANFIS modeling. *Int. J. Adv. Manuf. Technol.* **2014**, *74*, 531–537. [CrossRef]
- Çolak, O.; Kurbanoglu, C.; Kayacan, M.C. Milling surface roughness prediction using evolutionary programming methods. *Mater. Des.* **2007**, *28*, 657–666. [CrossRef]
- Hayajneh, M.; Tahat, M.S.; Bluhm, J. A Study of the Effects of Machining Parameters on the Surface Roughness in the End-Milling Process. *Jordan J. Mech. Ind. Eng.* **2007**, *1*, 1–5.
- Simunovic, K.; Simunovic, G.; Saric, T. Predicting the Surface Quality of Face Milled Aluminium Alloy Using a Multiple Regression Model and Numerical Optimization. *Meas. Sci. Rev.* **2013**, *13*, 265–272. [CrossRef]
- Yeganefar, A.; Niknam, S.A.; Asadi, R. The use of support vector machine, neural network, and regression analysis to predict and optimize surface roughness and cutting forces in milling. *Int. J. Adv. Manuf. Technol.* **2019**, *105*, 951–965. [CrossRef]
- Nguyen, H.T.; Hsu, Q.C. Surface Roughness Analysis in the Hard Milling of JIS SKD61 Alloy Steel. *Appl. Sci.* **2016**, *6*, 172. [CrossRef]
- Alauddin, M.; El Baradie, M.A.; Hashmi, M. Computer-aided analysis of a surface-roughness model for end milling. *J. Mater. Process. Technol.* **1995**, *55*, 123–127. [CrossRef]
- Philip, S.D.; Chandramohan, P.; Rajesh, P.K. Prediction of surface roughness in end milling operation of duplex stainless steel using response surface methodology. *J. Eng. Sci. Technol.* **2015**, *10*, 340–352.

16. Zhang, S.; Li, J.F.; Ding, T.C. Statistical Modeling of Surface Roughness in Hard Milling H13 Steel. *Mater. Sci. Forum* **2011**, 697–698, 61–66. [[CrossRef](#)]
17. Palanisamy, P.; Rajendran, I.; Shanmugasundaram, S. Prediction of tool wear using regression and ANN models in end-milling operation. *Int. J. Adv. Manuf. Technol.* **2008**, 37, 29–41. [[CrossRef](#)]
18. Xu, L.H.; Huang, C.Z.; Niu, J.H.; Wang, J.; Liu, H.L.; Wang, X.D. Prediction of cutting power and surface quality, and optimization of cutting parameters using new inference system in high-speed milling process. *Adv. Manuf.* **2021**, 9, 388–402. [[CrossRef](#)]
19. Gupta, A.; Singh, H.; Aggarwal, A. Taguchi-fuzzy multi output optimization (MOO) in high speed CNC turning of AISI P-20 tool steel. *Expert Syst. Appl.* **2011**, 38, 6822–6828. [[CrossRef](#)]
20. Yang, W.A.; Guo, Y.; Liao, W.H. Optimization of multi-pass face milling using a fuzzy particle swarm optimization algorithm. *Int. J. Adv. Manuf. Technol.* **2011**, 54, 45–57. [[CrossRef](#)]
21. Ströbel, R.; Mau, M.; Deucker, S.; Fleischer, J. *Training and Validation Dataset 2 of Milling Processes for Time Series Prediction*; Institut für Produktionstechnik (WBK): Karlsruhe, Germany, 2023. [[CrossRef](#)]
22. Ströbel, R.; Probst, Y.; Fleischer, J. *Training and Validation Dataset of Milling Processes for Time Series Prediction*; Institut für Produktionstechnik (WBK): Karlsruhe, Germany, 2023. [[CrossRef](#)]
23. Dijmarescu, M.R.; Dijmarescu, M.C.; Voiculescu, I.; Popovici, T.D.; Tarba, I.C. Study on the influence of cutting parameters on surface quality when machining a CoCrMo alloy. *IOP Conf. Ser. Mater. Sci. Eng.* **2018**, 400, 022020. [[CrossRef](#)]

**Disclaimer/Publisher’s Note:** The statements, opinions and data contained in all publications are solely those of the individual author(s) and contributor(s) and not of MDPI and/or the editor(s). MDPI and/or the editor(s) disclaim responsibility for any injury to people or property resulting from any ideas, methods, instructions or products referred to in the content.